

## Proton Coulomb Blockade Effect Involving Covalent Oxygen-Hydrogen Bond Switching

Yuwei Cao<sup>1</sup>, Wanqi Zhou,<sup>2</sup> Chun Shen,<sup>2</sup> Hu Qiu<sup>1,2,\*</sup> and Wanlin Guo<sup>2,†</sup>

<sup>1</sup>State Key Laboratory of Tribology, Department of Mechanical Engineering,  
Tsinghua University, Beijing 100084, China

<sup>2</sup>National Key Laboratory of Mechanics and Control for Aerospace Structures and  
Key Laboratory for Intelligent Nano Materials and Devices of the Ministry of Education,  
Institute for Frontier Science, Nanjing University of Aeronautics and  
Astronautics, Nanjing 210016, China

 (Received 8 October 2023; accepted 13 March 2024; published 29 April 2024)

Instead of the canonical Grotthuss mechanism, we show that a knock-on proton transport process is preferred between organic functional groups (e.g., -COOH and -OH) and adjacent water molecules in biological proton channel and synthetic nanopores through comprehensive quantum and classical molecular dynamics simulations. The knock-on process is accomplished by the switching of covalent O—H bonds of the functional group under externally applied electric fields. The proton transport through the synthetic nanopore exhibits nonlinear current-voltage characteristics, suggesting an unprecedented proton Coulomb blockade effect. These findings not only enhance the understanding of proton transport in nanoconfined systems but also pave the way for the design of a variety of proton-based nanofluidic devices.

DOI: [10.1103/PhysRevLett.132.188401](https://doi.org/10.1103/PhysRevLett.132.188401)

Proton transfer plays a pivotal role in many areas of biology, chemistry, and physics [1]. Typically, proton transport in bulk water occurs in a “hopping” manner along hydrogen bonds formed between neighboring water molecules [2–5], as depicted by the two-century-old Grotthuss mechanism [6,7]. Compared with the bulk system, protons usually move more rapidly within ordered hydrogen bond networks between water molecules in the two-dimensional nanoslits [8–12] and the interior of nanotubes [13–15]. In fact, proton transport along hydrogen bonds formed between organic functional groups and other entities (not limited to water molecules) is more universal and complex than that solely between water molecules. For instance, human voltage-gated proton channels (hHv1) conduct protons across cell membranes under the mediation by functional groups of pore-lining residues to regulate intracellular *pH*, and are widespread in human tissues such as innate and adaptive immune cells, cancer cells, and sperm [16–18]. Dysfunction of hHv1 proton channel has been implicated in many aspects of health and disease [19,20]. Therefore, it is important to know how this proton channel functions, especially how it conveys protons with the help of organic functional groups around the central pore. Parallel to these investigations, synthetic biomimetic proton channels functionalized with similar organic groups have been proposed, including designed channel proteins [21,22], covalent-organic frameworks, and metal-organic frameworks [23,24]. Molecular insights into the mechanism governing proton transfer in these biological and synthetic systems would be of fundamental scientific interest and beneficial to applications in enzyme catalysis

[25], proton separation technologies [26–28], nanofluidic memristors [29], and neuromorphic devices [30]. For instance, it is important to know whether novel proton transport behavior arises in these systems [31,32].

Here, we demonstrate via quantum and classical molecular dynamics (MD) simulations that proton transfer between water molecules and organic functional groups (e.g., -OH or -COOH) in the hHv1 proton channel or synthetic nanopores can adopt a knock-on manner, instead of conventional Grotthuss diffusion. We observe that the knock-on process occurs continuously in the synthetic nanopores at sufficiently large electric fields (i.e., absent at low fields). The resulting nonlinear current-voltage relationship suggests that the knock-on process is voltage dependent and mediated by a novel proton Coulomb blockade (CB) effect, the counterpart of the electronic [33–39] and ionic [40–46] CB. In addition, the proton CB involves the dynamic switching of O—H bonds, making it different from the ionic CB. These findings highlight the unique and rich behaviors of proton transport under nanoconfinement.

The open-state hHv1 proton channel, embedded in a 1-palmitoyl-2-oleoyl-sn-glycero-3-phosphorylcholine (POPC) lipid membrane solvated in 0.15 M NaCl solution, was used as the model system [Fig. 1(a); see Supplemental Material Sec. S1 [47] for details]. Prior to quantum mechanics/molecular mechanics (QM/MM) simulations, we conducted a 100 ns classical MD simulation to equilibrate the system, with the last 10 ns being collected for analysis. It is found that water molecules form continuous chains throughout the hHv1 channel, except in the

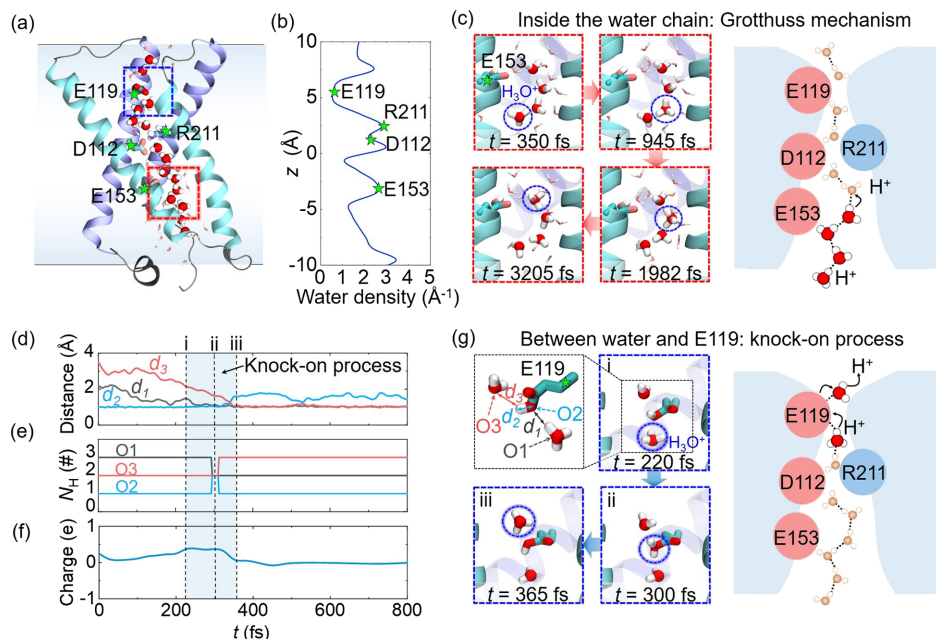


FIG. 1. Proton transport in the hHv1 proton channel. (a) Atomic model of the hHv1 proton channel. The hHv1 channel is shown as ribbons, with pore-lining residues displayed in licorice. A few water molecules and hydronium ions ( $\text{H}_3\text{O}^+$ ) inside the channel are shown by the VDW representation. (b) Density profile of water along the channel pore ( $z$  axis). (c) Snapshots from a QM/MM simulation illustrating the proton transport process along the water chain via the Grotthuss mechanism. The right panel shows a schematic of the Grotthuss mechanism. (d) Time evolution of the distances between hydrogen atoms and surrounding oxygen atoms [see the top left panel in (g) for definitions] that participate in the knock-on process of proton transfer. (e) Time evolution of the number of hydrogen atoms ( $N_{\text{H}}$ ) bonded to the oxygen atom of the E119 side chain (O2) and the oxygen atoms of two adjacent water molecules (O1 and O3). (f) Charge transfer between the E119 side chain and its surroundings during the knock-on process. (g) Snapshots from a QM/MM simulation showing the knock-on process of proton transport. The right panel shows a schematic of the knock-on process.

vicinity of the E119 residue [Fig. 1(a)]. This observation is in line with the extremely low water density around E119 [Fig. 1(b)]. Subsequently, we conducted two groups of QM/MM simulations to exploit proton transport between (i) adjacent water molecules in the water chain and (ii) a water molecule and the side chain of E119. In the first group of QM/MM simulations, a single proton was initially added to a randomly picked water molecule in the water chain [away from E119; see the red rectangle in Fig. 1(a)], forming a  $\text{H}_3\text{O}^+$ . Subsequently, a transmembrane voltage of 150 mV was applied to the system. As expected, this proton hops between neighboring water molecules along the water chain [see simulation snapshots in Fig. 1(c)], a scenario that can be well described by the canonical Grotthuss mechanism.

In the second group of QM/MM simulations, a proton was initially added to a water molecule in close proximity to the E119 residue, which is in a protonated state due to the acidic environment inside the channel [18] [see the blue rectangle in Fig. 1(a)]. In contrast to the Grotthuss diffusion, a knock-on process is clearly seen for proton transfer between E119 and adjacent water molecules under a transmembrane voltage of 150 mV [see Figs. 1(d)–1(f), simulation snapshots in Fig. 1(g), and movie S1 [47] of the Supplemental Material]. During this process, the distance of the added proton to the oxygen atom in the E119 side

chain ( $d_1$ ) gradually decreases until it reaches a stable value of  $\sim 1$  Å, corresponding to the formation of an O–H bond. Almost at the same time ( $\sim 50$  fs later), the hydrogen atom originally bonded to the E119 oxygen is knocked off by the incoming proton, jumping to another water molecule, as indicated by its increasing distance to the E119 oxygen ( $d_2$ ) and decreasing distance to the water oxygen [ $d_3$ ; Fig. 1(d)]. Likewise, this process can also be characterized by the change in the number of hydrogen atoms bonded to the three oxygen atoms [Fig. 1(e)]. At the same time, a charge transfer between the side chain of residue E119 and the environment is also detected [Fig. 1(f)]. Such a proton transport process is in spirit similar to the knock-on phenomena observed in biological potassium and sodium ion channels [83–85]. The above results show that both the Grotthuss [Fig. 1(c)] and knock-on [Fig. 1(g)] mechanisms are involved in proton transport in the hHv1 channel.

Reproducing the elegant transport properties displayed by biological ion or proton channels in synthetic nanopore systems is highly desirable due to their great technical potential [86–88]. We will demonstrate below that the knock-on mechanism is transferable to a series of synthetic nanopores, functionalized with similar organic groups as in biological proton channels. We first considered a 0.3 nm wide (effective diameter) graphene nanopore solvated in proton-containing solutions [Fig. 2(a)], with its edge

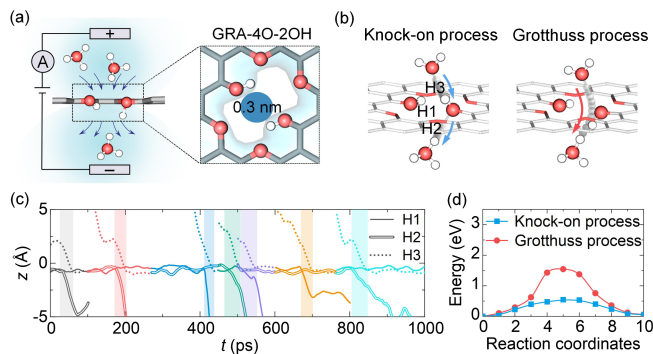


FIG. 2. Knock-on proton transport through functionalized synthetic nanopores. (a) Proton transport through a functionalized graphene nanopore. The right panel shows the top view of the GRA-4O-2OH graphene nanopore, terminated with four oxygen atoms (red spheres) and two hydroxyl groups (red and white spheres). (b) Schematic of the knock-on and Grotthuss processes. (c) Positions of hydrogen atoms of hydroxyl groups (H1 and H2) and a proton (H3) involved in the knock-on process. Note that many knock-on processes under an electric field of 1.3 V/nm, shown in different colors, are identified in the simulation trajectory. (d) Energy barriers of proton penetration through the nanopore via the Grotthuss and knock-on processes, calculated with the DFT-NEB method.

terminated by four oxygen atoms and two hydroxyl groups (GRA-4O-2OH). The hydroxyl groups (-OH) act as both proton receptors and donors (same role as residue E119 in the biological proton channel) and the negatively charged ether groups (-O) are responsible for attracting protons. To acquire adequate proton permeation events and a convergent current through the pore, a sufficiently long timescale is usually needed in simulations. Considering the extremely high computational cost of the aforementioned QM/MM simulations, we chose to conduct classical MD simulations with reactive force field (ReaxFF) potential [48] (see Supplemental Material Sec. S2 [47] for details). Similar to the situation in the E119 region of the hHv1 channel, water molecules are unable to form a continuous chain across the synthetic pore, and the knock-on proton transport is found to occur frequently between hydroxyl groups and adjacent water molecules [Fig. 2(b) and movie S2 [47] of the Supplemental Material]. In addition, the occurrence of the knock-on process is voltage dependent: it is only seen in electric fields ( $E$ ) higher than 0.8 V/nm; the stronger the field, the more frequently the knock-on process takes place [see Fig. 2(c) and Fig. S1 [47]]. During a typical knock-on process at 1.3 V/nm, a proton (H3) in the form of  $\text{H}_3\text{O}^+$  first approaches the pore from the above, knocks off one of the hydrogen atoms (either H1 or H2) of hydroxyl groups and sends it to a water molecule below the pore, forming a new  $\text{H}_3\text{O}^+$  [see Figs. 2(b) and 2(c)]. In other words, the original O-H bond of the hydroxyl group is broken and a new O-H bond is formed between the proton H3 and the retained hydroxyl oxygen.

We further compared the energy barriers of the Grotthuss and knock-on processes using the density functional

theory-based nudged elastic band (DFT-NEB) method [89] (see Supplemental Material Sec. S3 [47] for details). Different from the knock-on process, whereby the hydroxyl group accepts a proton from an upper  $\text{H}_3\text{O}^+$  and simultaneously donates a hydrogen atom to a lower  $\text{H}_2\text{O}$ , the Grotthuss process involves stepwise proton hopping between three sites, from the upper  $\text{H}_3\text{O}^+$  to the hydroxyl group and finally to the lower  $\text{H}_2\text{O}$  [Fig. 2(b)]. The calculated energy barrier for the knock-on process is  $\sim 0.54$  eV, approximately one-third of that associated with the Grotthuss process [ $\sim 1.54$  eV; Fig. 2(d)]. Therefore, the knock-on process represents an energy-favorable way for proton transport through the synthetic nanopore, consistent with our above simulation results. Our additional calculations show that the knock-on mechanism is also the preferred one in many other organic group functionalized nanopores (Fig. S2 [47]), e.g., those terminated with a single hydroxyl group (GRA-5O-OH) or a carboxyl group (GRA-5O-COOH). The reason why proton conduction does not occur via the Grotthuss mechanism is presumably related to the fact that the -OH group at the pore edge is not in favor of accepting another H (proton), as found in our additional *ab initio* molecular dynamics (AIMD) simulations (Fig. S3 and see Supplemental Material Sec. S4 for details [47]).

To further exploit the voltage dependence of knock-on proton transport, we determined the current-voltage ( $I$ - $V$ ) response by calculating the current through the synthetic nanopore at a series of field strengths. Figure 3(a) shows typical  $I$ - $V$  curves of proton transport through the

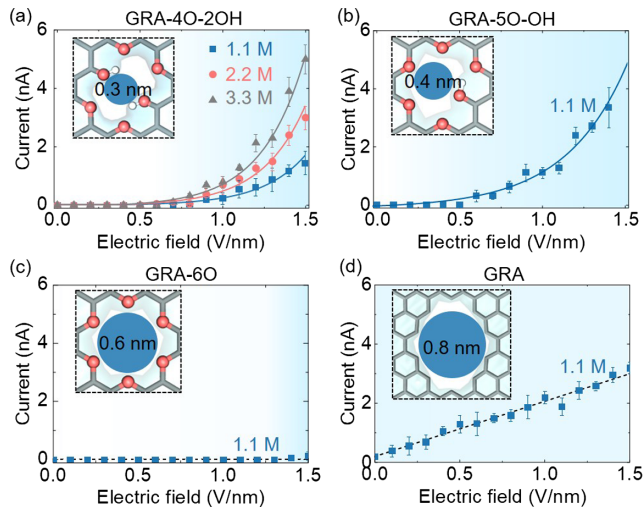


FIG. 3. Voltage dependence of proton transport through synthetic nanopores. (a) Recorded current through the GRA-4O-2OH nanopore as a function of the electric field at different proton concentrations. (b),(c),(d) Recorded currents through an oxygen-terminated pore (GRA-6O), a hydroxyl-terminated pore (GRA-5O-OH) and a pristine pore (GRA) as a function of the electric field at a proton concentration of 1.1 M. In (a) and (b), the solid lines show the results obtained with Eq. (2), while in (c) and (d), the dashed lines indicate linear fitting to the simulation data. The error bars represent the standard deviations of four sub-trajectories out of a complete MD trajectory.

GRA-4O-2OH nanopore (0.3 nm) at varying proton concentrations (1.1–3.3 M). The  $I$ - $V$  curve exhibits a striking nonlinear feature, along with a prominent blocked gap of about 0.8 V/nm [Fig. 3(a)]. In other words, when  $E < 0.8$  V/nm, a nearly vanishing current is detected as no knock-on proton transport occurs; when  $E > 0.8$  V/nm, the proton current gradually increases with the electric field (i.e., more proton permeation events take place). It is also found that the use of a higher proton concentration results in a larger current but does not significantly change the width of the blocked gap [Fig. 3(a)]. A similar nonlinear  $I$ - $V$  curve is observed in a graphene nanopore terminated by five oxygen atoms and one hydroxyl group (GRA-5O-OH, 0.4 nm), albeit with a smaller blocked gap [Fig. 3(b)]. In a nanopore terminated with only oxygen atoms (GRA-6O, 0.6 nm), the proton current is always zero at electric fields as high as 1.3 V/nm [Fig. 3(c)]. This is because knock-on proton transport cannot take place in the absence of the hydroxyl group. For a sufficiently wide graphene nanopore, no matter with the hydroxyl group (GRA-12O-OH, 0.9 nm; see Fig. S4 [47]) or not [GRA, 0.8 nm; see Fig. 3(d)], protons are transported along the continuous water chain through the pore via the Grotthuss mechanism. In this situation, the  $I$ - $V$  curve exhibits a linear Ohmic response [Fig. 3(d)]. These results suggest that both a suitable pore size and the presence of organic groups at the pore edge are critical for enabling knock-on proton transport.

The nonlinear behaviors of the  $I$ - $V$  curves, in particular the blocked gap at low biases, act as a signature for Coulomb blockade, a single-electron or ion transport effect widely seen for electron transport in quantum dots [33–39] or ion transport through subnanometer pores [40–46]. We suggest below a single-proton transport mechanism to account for the proton CB effect in the proton transport process. The nanopore system can be approximately described with a simple circuit model [Fig. 4(a)], whereby the nanopore itself can be treated as a quantum dot (QD) possessing a small capacitance ( $C$ ) in addition to its resistance ( $R$ ). A single proton entering the nanopore results in a charging energy  $E_{\text{elec}} = (e^2/2C) + (Qe/C)$  as a consequence of electrostatic interactions [42], where  $Q$  is the initial charge of the capacitor and  $e$  is the elementary charge. When the capacitance is sufficiently small, a very high charging energy has to be overcome to initiate proton transfer [see the top panel in Fig. 4(b)]. In the present system,  $Q$  is determined as the sum of partial charges surrounding the nanopore ( $-0.14e$  for the GRA-4O-2OH nanopore; see Supplemental Material Sec. S5 [47] for details).  $C$  is given by  $4\epsilon\epsilon_0\pi r^2/L$  ( $r$  is the pore radius,  $L$  is the membrane thickness,  $\epsilon_0$  and  $\epsilon$  are dielectric constants of vacuum and water, respectively). For very small nanopores ( $r \leq 0.35$  nm),  $\epsilon$  is a distance-dependent screening factor [49] (see Supplemental Material Sec. S6 [47] for details).

In addition to the electrostatic interaction, another key factor that prevents proton penetration is the energy barrier

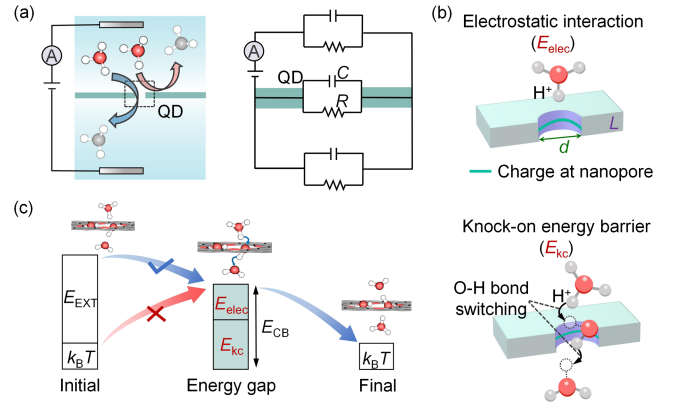


FIG. 4. The underlying mechanism for the proton CB effect. (a) Equivalent circuit for the nanopore system. An analogy to quantum dots (QDs) is used to describe the nanopore for proton penetration. (b) The top panel shows a proton accompanied by charging energy ( $E_{\text{elec}}$ ) approaching the nanopore. The bottom panel shows the energy barrier  $E_{\text{kc}}$  of the knock-on proton transport process involving the breaking and formation of O–H covalent bonds. The green circle represents the charge at the nanopore. (c) Equivalent energy-level diagram for proton CB. When the energy gap ( $E_{\text{CB}}$ ) is higher than the thermal energy ( $k_{\text{B}}T$ ), proton conduction is suppressed (blocked state). A buildup in an electric field ( $E_{\text{EXT}}$ ) above  $E_{\text{CB}}$  allows for proton conduction (open state).

$E_{\text{kc}}$  of the knock-on process involving the switching of O–H bonds [see the bottom panel in Fig. 4(b),  $E_{\text{kc}}$  for different nanopores are listed in Table S1 [47] of the Supplemental Material]. Altogether, the sum of the electrostatic interaction and the knock-on energy barrier forms an energy gap  $E_{\text{CB}}$  hindering proton transfer:

$$E_{\text{CB}} = E_{\text{elec}} + E_{\text{kc}}. \quad (1)$$

Figure 4(c) sketches a schematic of the energy diagram involved in the above process. If  $E_{\text{CB}}$  is much larger than the thermal energy of a proton at room temperature ( $k_{\text{B}}T$ , with  $T = 298$  K), the CB phenomenon would arise, suppressing the proton transport. Under an external electric field  $E$ , the proton gains additional energy  $E_{\text{EXT}} = eEL$  to promote its transfer. When this energy rises above the energy gap, proton penetration is expected to occur. Based on the energy diagram of proton transport, we can employ the modified Eyring theory to describe the observed nonlinear  $I$ - $V$  curves of proton transport [50]:

$$I = c_0 A \frac{\exp\left[\frac{B}{n}(E_{\text{EXT}} - E_{\text{CB}})\right] - 1}{\exp[B(E_{\text{EXT}} - E_{\text{CB}})] - 1} [\exp(BE_{\text{EXT}}) - 1], \quad (2)$$

where  $c_0$  is the proton concentration,  $A$  and  $B$  are parameters that depend on the rate constant for proton transfer and temperature, respectively.  $n$  represents the number of transition barriers for proton transport (see Supplemental Material Sec. S7 for details [47]). This

equation fits well for the nonlinear  $I$ - $V$  curves [41,51] of the GRA-4O-2OH [Fig. 3(a)] and GRA-5O-OH [Fig. 3(b)] nanopores.

It is also worth noting that the proton-proton electrostatic interaction in the pore is neglected in the above derivation since all the nanopores studied are found to be able to convey protons one at a time. Furthermore, other factors, such as changes in the strength of the internal electric field in nanopores in response to external electric fields and  $pH$  under various proton concentrations [45,90,91], may also influence proton transport. A more detailed understanding of the impact of these issues on proton transport requires further computational or theoretical studies.

Although the proton CB yields similar  $I$ - $V$  curves as the ionic CB, the underlying transport mechanism is quite different. Specifically, the knock-on energy barrier  $E_{kc}$  of proton CB involves the switching of the covalent O—H bonds, such that the proton CB cannot be explained alone by electrostatics. Obviously, this barrier is not involved in the ionic CB where the dehydration effect and Coulomb energy govern ion transport [41,45]. In other words, the proton CB manifests as a chemical-physical process accompanied with the switching of O—H bonds, making it different from the ionic CB.

In summary, we have demonstrated by comprehensive quantum and classical molecular dynamics simulations that knock-on proton transport can occur in the biological proton channel and synthetic nanopores. This process is found to be strongly voltage dependent in synthetic nanopores, manifesting as nonlinear current-voltage characteristics and a voltage gap at low biases. These two features suggest that the knock-on proton transport results in the CB effect, a consequence of the single-proton charging energy and the knock-on energy barrier. In sharp contrast to the ionic CB, the knock-on process is accomplished by the switching of the covalent O—H bonds. This novel proton transport mechanism in nanoconfined spaces is of particular significance to understanding the functioning of biological proton channels and opens up the possibility of developing a wide range of proton-based nanofluidic devices.

This work was supported by National Natural Science Foundation of China (T2293691, 12172170, 12322213, 12150002), National Key Research and Development Program of China (2019YFA0705400), Natural Science Foundation of Jiangsu Province (BK20212008, BK20221476, BK20230029), the Fundamental Research Funds for the Central Universities (NC2023001, NJ2023002) and the Fund of Prospective Layout of Scientific Research for NUAA (Nanjing University of Aeronautics and Astronautics). The authors thank Professor J. X. Zhou, Dr. J. L. Zhu, Dr. C. C. Zhou, and Dr. B. Jin for helpful discussions.

\*Corresponding author: qiuhu@nuaa.edu.cn

†Corresponding author: wlguo@nuaa.edu.cn

- [1] J. T. Hynes, *Nature (London)* **446**, 271 (2007).
- [2] C. T. Wolke, J. A. Fournier, L. C. Dzugan, M. R. Fagiani, T. T. Odbadrakh, H. Knorke, K. D. Jordan, A. B. McCoy, K. R. Asmis, and M. A. Johnson, *Science* **354**, 1131 (2016).
- [3] M. Thämer, L. De Marco, K. Ramasesha, A. Mandal, and A. Tokmakoff, *Science* **350**, 78 (2015).
- [4] S. Woutersen and H. J. Bakker, *Phys. Rev. Lett.* **96**, 138305 (2006).
- [5] K. R. Asmis, N. L. Pivonka, G. Santambrogio, M. Brummer, C. Kaposta, and D. M. Neumark, *Science* **299**, 1375 (2003).
- [6] D. Marx, *Chem. Phys. Chem.* **7**, 1848 (2006).
- [7] N. Agmon, *Chem. Phys. Lett.* **244**, 456 (1995).
- [8] D. Munoz-Santiburcio and D. Marx, *Phys. Rev. Lett.* **119**, 056002 (2017).
- [9] S. Imoto and D. Marx, *Phys. Rev. Lett.* **125**, 086001 (2020).
- [10] M. Zakertabrizi, E. Hosseini, A. Habibnejad Korayem, and A. Razmjou, *Adv. Mater. Technol.* **6**, 2001049 (2021).
- [11] A. K. Geim, *Nano Lett.* **21**, 6356 (2021).
- [12] V. Kapil, C. Schran, A. Zen, J. Chen, C. J. Pickard, and A. Michaelides, *Nature (London)* **609**, 512 (2022).
- [13] C. Dellago, M. M. Naor, and G. Hummer, *Phys. Rev. Lett.* **90**, 105902 (2003).
- [14] D. J. Mann and M. D. Halls, *Phys. Rev. Lett.* **90**, 195503 (2003).
- [15] C. Dellago and G. Hummer, *Phys. Rev. Lett.* **97**, 245901 (2006).
- [16] I. S. Ramsey, Y. Mokrab, I. Carvacho, Z. A. Sands, M. S. Sansom, and D. E. Clapham, *Nat. Struct. Mol. Biol.* **17**, 869 (2010).
- [17] B. Musset, S. M. Smith, S. Rajan, D. Morgan, V. V. Cherny, and T. E. DeCoursey, *Nature (London)* **480**, 273 (2011).
- [18] D. Boytsov, S. Brescia, G. Chaves, S. Koeffler, C. Hanneschlaeger, C. Siligan, N. Goessweiner-Mohr, B. Musset, and P. Pohl, *Small* **19**, 2205968 (2023).
- [19] L.-J. Wu, G. Wu, M. R. A. Sharif, A. Baker, Y. Jia, F. H. Fahey, H. R. Luo, E. P. Feener, and D. E. Clapham, *Nat. Neurosci.* **15**, 565 (2012).
- [20] A. Fernández, A. Pupo, K. Mena-Ulecia, and C. Gonzalez, *Mol. Pharmacol.* **90**, 385 (2016).
- [21] H. T. Kratochvil, L. C. Watkins, M. Mravic, J. L. Thomaston, J. M. Nicoludis, N. H. Somberg, L. Liu, M. Hong, G. A. Voth, and W. F. DeGrado, *Nat. Chem.* **15**, 1012 (2023).
- [22] T. Yan, S. Liu, J. Xu, H. Sun, S. Yu, and J. Liu, *Nano Lett.* **21**, 10462 (2021).
- [23] F. Xu, Y. Wang, C. Lian, and Z. Xu, *J. Membr. Sci.* **648**, 120361 (2022).
- [24] X. Li, H. Zhang, H. Yu, J. Xia, Y.-B. Zhu, H.-A. Wu, J. Hou, J. Lu, R. Ou, C. D. Easton *et al.*, *Adv. Mater.* **32**, 2001777 (2020).
- [25] L. Masgrau, A. Roujeinikova, L. O. Johannissen, P. Hothi, J. Basran, K. E. Ranaghan, A. J. Mulholland, M. J. Sutcliffe, N. S. Scrutton, and D. Leys, *Science* **312**, 237 (2006).
- [26] K. Gopinadhan, S. Hu, A. Esfandiari, M. Lozada-Hidalgo, F. Wang, Q. Yang, A. Tyurnina, A. Keerthi, B. Radha, and A. Geim, *Science* **363**, 145 (2019).

- [27] L. Mogg, S. Zhang, G.-P. Hao, K. Gopinadhan, D. Barry, B. Liu, H. Cheng, A. Geim, and M. Lozada-Hidalgo, *Nat. Commun.* **10**, 4243 (2019).
- [28] S. Hu, M. Lozada-Hidalgo, F. Wang, A. Mishchenko, F. Schedin, R. R. Nair, E. Hill, D. Boukhvalov, M. Katsnelson, R. A. Dryfe *et al.*, *Nature (London)* **516**, 227 (2014).
- [29] P. Robin, T. Emmerich, A. Ismail, A. Niguès, Y. You, G.-H. Nam, A. Keerthi, A. Siria, A. Geim, B. Radha *et al.*, *Science* **379**, 161 (2023).
- [30] T. Xiong, C. Li, X. He, B. Xie, J. Zong, Y. Jiang, W. Ma, F. Wu, J. Fei, P. Yu *et al.*, *Science* **379**, 156 (2023).
- [31] L. Shi, Z. Ying, A. Xu, and Y. Cheng, *Chem. Mater.* **32**, 6062 (2020).
- [32] J. Comtet, B. Grosjean, E. Glushkov, A. Avsar, K. Watanabe, T. Taniguchi, R. Vuilleumier, M.-L. Bocquet, and A. Radenovic, *Nat. Nanotechnol.* **15**, 598 (2020).
- [33] C. W. J. Beenakker, *Phys. Rev. B* **44**, 1646 (1991).
- [34] D. Averin and K. Likharev, *J. Low Temp. Phys.* **62**, 345 (1986).
- [35] T. A. Fulton and G. J. Dolan, *Phys. Rev. Lett.* **59**, 109 (1987).
- [36] O. Model, *Sov. Phys. JETP* **36**, 747 (1973), [http://jetp.ras.ru/cgi-bin/dn/e\\_036\\_04\\_0747.pdf](http://jetp.ras.ru/cgi-bin/dn/e_036_04_0747.pdf).
- [37] K. Chan, P. Lee, and J. Dai, *Appl. Phys. Lett.* **92**, 143117 (2008).
- [38] R. Wilkins, E. Ben-Jacob, and R. C. Jaklevic, *Phys. Rev. Lett.* **63**, 801 (1989).
- [39] M. Yoshihira, S. Moriyama, H. Guerin, Y. Ochi, H. Kura, T. Ogawa, T. Sato, and H. Maki, *Appl. Phys. Lett.* **102**, 203117 (2013).
- [40] N. Kavokine, S. Marbach, A. Siria, and L. Bocquet, *Nat. Nanotechnol.* **14**, 573 (2019).
- [41] F. Chen, Z. Gu, C. Zhao, Y. Chen, X. Jiang, Z. He, Y. Lu, R. Zhou, and J. Feng, *Matter* **4**, 2378 (2021).
- [42] I. K. Kaufman, P. V. McClintock, and R. Eisenberg, *New J. Phys.* **17**, 083021 (2015).
- [43] A. Kamenev, J. Zhang, A. Larkin, and B. Shklovskii, *Phys. A* **359**, 129 (2006).
- [44] S. Zhang, L. Fu, and Y. Xie, [arXiv:2304.13355](https://arxiv.org/abs/2304.13355).
- [45] J. Feng, K. Liu, M. Graf, D. Dumcenco, A. Kis, M. Di Ventura, and A. Radenovic, *Nat. Mater.* **15**, 850 (2016).
- [46] Y. Xie, D. Shi, W. Wang, and Z. Wang, [arXiv:2211.07973](https://arxiv.org/abs/2211.07973).
- [47] See Supplemental Material at <http://link.aps.org/supplemental/10.1103/PhysRevLett.132.188401>, which includes Refs. [41,48–82], for a detailed description of simulation methods, additional results and discussion, as well as supplemental Figs. S1–S5, Tables S1-S4 and Movies S1-S2.
- [48] L. Liu, Y. Liu, S. V. Zybin, H. Sun, and W. A. Goddard III, *J. Phys. Chem. A* **115**, 11016 (2011).
- [49] A. Laio and V. Torre, *Biophys. J.* **76**, 129 (1999).
- [50] J. Woodbury, *Adv. Chem. Phys.* **XVI**, 601 (1971).
- [51] S. Sahu, J. Elenewski, C. Rohmann, and M. Zwolak, *Sci. Adv.* **5**, eaaw5478 (2019).
- [52] A. D. Geragotelis, M. L. Wood, H. Göddeke, L. Hong, P. D. Webster, E. K. Wong, J. A. Freites, F. Tombola, and D. J. Tobias, *Proc. Natl. Acad. Sci. U.S.A.* **117**, 13490 (2020).
- [53] S. Jo, T. Kim, V. G. Iyer, and W. Im, *J. Comput. Chem.* **29**, 1859 (2008).
- [54] H. Li, A. D. Robertson, and J. H. Jensen, *Proteins* **61**, 704 (2005).
- [55] S. C. van Keulen, E. Gianti, V. Carnevale, M. L. Klein, U. Rothlisberger, and L. Delemotte, *J. Phys. Chem. B* **121**, 3340 (2017).
- [56] M. Lee, C. Bai, M. Feliks, R. Alhadeff, and A. Warshel, *Proc. Natl. Acad. Sci. U.S.A.* **115**, 10321 (2018).
- [57] J. C. Phillips, D. J. Hardy, J. D. Maia, J. E. Stone, J. V. Ribeiro, R. C. Bernardi, R. Buch, G. Fiorin, J. Hémin, W. Jiang *et al.*, *J. Chem. Phys.* **153**, 044130 (2020).
- [58] J. B. Klauda, R. M. Venable, J. A. Freites, J. W. O'Connor, D. J. Tobias, C. Mondragon-Ramirez, I. Vorobyov, A. D. MacKerell Jr, and R. W. Pastor, *J. Phys. Chem. B* **114**, 7830 (2010).
- [59] R. B. Best, X. Zhu, J. Shim, P. E. Lopes, J. Mittal, M. Feig, and A. D. MacKerell Jr, *J. Chem. Theory Comput.* **8**, 3257 (2012).
- [60] D. Beglov and B. Roux, *J. Chem. Phys.* **100**, 9050 (1994).
- [61] W. L. Jorgensen, J. Chandrasekhar, J. D. Madura, R. W. Impey, and M. L. Klein, *J. Chem. Phys.* **79**, 926 (1983).
- [62] M. C. Melo, R. C. Bernardi, T. Rudack, M. Scheurer, C. Riplinger, J. C. Phillips, J. D. Maia, G. B. Rocha, J. V. Ribeiro, J. E. Stone *et al.*, *Nat. Methods* **15**, 351 (2018).
- [63] J. J. Stewart, *J. Comput. Aid. Mol. Des.* **4**, 1 (1990).
- [64] H. Lin and D. G. Truhlar, *J. Phys. Chem. A* **109**, 3991 (2005).
- [65] W. Humphrey, A. Dalke, and K. Schulten, *J. Mol. Graphics* **14**, 33 (1996).
- [66] G. Kresse and J. Furthmüller, *Comput. Mater. Sci.* **6**, 15 (1996).
- [67] S. Plimpton, *J. Comput. Phys.* **117**, 1 (1995).
- [68] A. P. Thompson, H. M. Aktulga, R. Berger, D. S. Bolintineanu, W. M. Brown, P. S. Crozier, P. J. in't Veld, A. Kohlmeyer, S. G. Moore, T. D. Nguyen *et al.*, *Comput. Phys. Commun.* **271**, 108171 (2022).
- [69] S. Nosé, *J. Chem. Phys.* **81**, 511 (1984).
- [70] W. G. Hoover, *Phys. Rev. A* **31**, 1695 (1985).
- [71] M. Sobrino Fernandez Mario, M. Neek-Amal, and F. M. Peeters, *Phys. Rev. B* **92**, 245428 (2015).
- [72] P. E. Blöchl, *Phys. Rev. B* **50**, 17953 (1994).
- [73] J. P. Perdew, K. Burke, and M. Ernzerhof, *Phys. Rev. Lett.* **77**, 3865 (1996).
- [74] J. Hutter, M. Iannuzzi, F. Schiffmann, and J. VandeVondele, *Wiley Interdiscip. Rev.-Comput. Mol. Sci.* **4**, 15 (2014).
- [75] J. VandeVondele and J. Hutter, *J. Chem. Phys.* **127**, 114105 (2007).
- [76] M. Krack, *Theor. Chem. Acc.* **114**, 145 (2005).
- [77] C. Hartwigsen, S. Goedecker, and J. Hutter, *Phys. Rev. B* **58**, 3641 (1998).
- [78] S. Goedecker, M. Teter, and J. Hutter, *Phys. Rev. B* **54**, 1703 (1996).
- [79] S. Grimme, S. Ehrlich, and L. Goerigk, *J. Comput. Chem.* **32**, 1456 (2011).
- [80] S. Grimme, J. Antony, S. Ehrlich, and H. Krieg, *J. Chem. Phys.* **132**, 154104 (2010).
- [81] M. Frisch, G. Trucks, H. B. Schlegel, G. Scuseria, M. Robb, J. Cheeseman, G. Scalmani, V. Barone, G. Petersson, H. Nakatsuji *et al.*, *Gaussian 16* (2016), <https://gaussian.com/g16main/>.

- [82] C. M. Breneman and K. B. Wiberg, *J. Comput. Chem.* **11**, 361 (1990).
- [83] W. Kopec, D. A. Köpfer, O. N. Vickery, A. S. Bondarenko, T. L. Jansen, B. L. De Groot, and U. Zachariae, *Nat. Chem.* **10**, 813 (2018).
- [84] D. A. Köpfer, C. Song, T. Gruene, G. M. Sheldrick, U. Zachariae, and B. L. de Groot, *Science* **346**, 352 (2014).
- [85] L. Liang, Z. Zhang, H. Wang, J.-W. Shen, and Z. Kong, *Int. J. Biol. Macromol.* **188**, 369 (2021).
- [86] I. Andrei and M. Barboiu, *Biomolecules* **12**, 1473 (2022).
- [87] P. Choi, N. H. Jalani, and R. Datta, *J. Electrochem. Soc.* **152**, E123 (2005).
- [88] L. Wu, Z. Zhang, J. Ran, D. Zhou, C. Li, and T. Xu, *Phys. Chem. Chem. Phys.* **15**, 4870 (2013).
- [89] G. Kresse and J. Furthmüller, *Phys. Rev. B* **54**, 11169 (1996).
- [90] M. Heiranian, A. B. Farimani, and N. R. Aluru, *Nat. Commun.* **6**, 8616 (2015).
- [91] X. Jiang, C. Zhao, Y. Noh, Y. Xu, Y. Chen, F. Chen, L. Ma, W. Ren, N. R. Aluru, and J. Feng, *Sci. Adv.* **8**, eabj2510 (2022).